eXPRESS Polymer Letters Vol.15, No.11 (2021) 1019–1031
Available online at www.expresspolymlett.com
https://doi.org/10.3144/expresspolymlett.2021.82

Scalable preparation of ultrathin porous polyurethane membrane-based triboelectric nanogenerator for mechanical energy harvesting

M. R. Gokana[1], *C-M. Wu*[1*], *U. Reddicherla*[2], *K. G. Motora*[1]

[1]Department of Materials Science and Engineering, National Taiwan University of Science and Technology, Keelung Road, 10607 Taipei, Taiwan, R. O. C.
[2]Department of Chemistry, University of Delhi, 110007 Delhi, India

Received 26 April 2021; accepted in revised form 18 June 2021

Abstract. Scalable preparation of flexible, porous, and microstructure membrane for triboelectric nanogenerators (TENGs) with controllable thickness and high contact surface area using cost-effective methods is still a great challenge. Herein, we developed a novel, cost-effective, and scalable fabrication procedure for the preparation of a lightweight, flexible, thin, and porous polyurethane (PU) membrane for a TENG device. Importantly, the thickness and pore size of the PU membrane can be tuned easily. The PU-based TENG device fabricated with a porous PU membrane of 5 μm thickness and 15 μm pore size (PU-5-15) generated a maximum peak to peak output voltage was 58.5 V with a corresponding peak to peak current was 1.37 μA at 4 N and power density of 9.7 mW/m^2. The device was systematically used to energize 24 green commercial light-emitting diodes (LEDs) in brighter condition connected in series and to turn on the LCD of a portable timer clock within 51 s and glow for 1 s after 187 taps. The developed TENG device also exhibited stable cyclic charging and discharging property that is very important for real applications. Furthermore, the energy-harvesting performance of the device was also tested with human body movements. The developed industrially compatible method is very easy and convenient, and mass production is possible. Compared to other studies, in this novel study, we achieved a higher electrical performance at the desired lower thickness for the porous PU membrane-based TENG device. The developed fabrication method will pave the way for the facile and scalable industrial processing of PU membranes for energy-harvesting applications.

Keywords: *polymer membranes, polyurethane, energy harvesting, triboelectric nanogenerator, coatings*

1. Introduction

Over the past few years, energy harvesting and storage have been regarded as important for the survival, wellbeing, and social evolution of human beings [1–6]. Cost-effective, environment-friendly energy harvesting generators, energy storage devices, and novel power sources are in high demand owing to the rapid proliferation and development of wearable sensors [7–13], the internet of things (IoT), wireless sensing nodes, microelectronics, flexible electronics, structural health-monitoring devices, environmental-sensing devices, and artificial intelligence devices [14–18]. On the other hand, energy crisis and environmental pollution problems are the most severe threats to humankind due to the excessive use of fossil fuel and coal power plant engines as traditional and conventional power sources. Since the 19th century, fossil fuel is the primary source of energy around the globe. The growing population of the world significantly depends on fossil fuels for their daily, scientific, and technological activities without considering their toxic impact on humans, animals, and the environment [19–23]. Owing to the over usage of fossil fuels, they are also rapidly depleting day by day.

*Corresponding author, e-mail: cmwu@mail.ntust.edu.tw
© BME-PT

Moreover, power and energy consumption of microelectronics and energy storage devices exhibits an increasing trend as the number of unit consumption has rapidly increased at an overwhelming rate, which in turn leads to the difficult task of replacing or recharging a vast number of batteries. Nevertheless, renewable and sustainable energies might be used as a possible alternative to overcome these problems, but these are not sufficient to support and satisfy the energy crisis for the current and coming decades [1, 3, 4, 15].

To overcome and solve these global issues, it is essential to develop safe and convenient energy-harvesting, generating, and storage technologies [24–27]. By considering all these issues, scientists have started developing advanced energy-harvesting and storage technologies from waste energy sources as possible and satisfactory substitutes for the abovementioned issues. In this regard, nanogenerators (NGs) have emerged as sustainable, user-friendly, and environment-friendly alternatives by converting mechanical energy into electricity [2, 7–10, 14, 16, 19–23]. These will play the main role in the conversion of ambient energies into electricity through different energy conversion processes, such as piezoelectric, electromagnetic, triboelectric, pyroelectric, and thermoelectric effects. Specifically, triboelectric nanogenerators (TENGs) and their hybrids have been extensively used for the conversion of vibrational, rotational, and mechanical energies into electricity. It is worth mentioning that TENG is significantly suitable for low amplitude, low frequency, and microenergy systems with various mechanical motions, owing to its different working modes (viz single-electrode mode, contact-separation mode, free-standing mode, and lateral sliding mode), a wide range of raw materials, ease of preparation, the potential to power portable electronic gadgets and abundant structure design [19, 22, 28–31]. Recently, new avenues have been laid down to bring the potential technological advancements in terms of multifunctionality and miniaturization for energy-harvesting and energy storage self-powered applications. On the other hand, to meet the requirements for some special applications, all parts of the TENG device must be flexible and stretchable [32–35].

Fabrication of porous polymer membranes with highly flexible features is very important for the current generation as they have attained overwhelming attention in self-powered NG based energy harvesting devices, supercapacitors, robotics, actuators, electronic gadgets, bionic skin, touch screens, and fuel cells [29, 36–38]. A porous, stretchable TENG with a flexible friction layer can be fabricated using flexible materials such as silicone rubber, polyurethane (PU), and polydimethylsiloxane (PDMS) [39-41]. Furthermore, to achieve the electrical output performance of the TENG device, the membranes were usually made of metallic materials lacking stretchability [42]. However, it is still challenging to develop porous, stretchable, flexible, and mass production of thin polymer membranes with controllable thickness and pore size using cost-effective methods. Several techniques such as lithography, photolithography, inductively coupled plasma etching, reactive ion etching, thermal imprint lithography, screen printing, and 3D printing have been proposed and developed to fabricate stretchable, flexible, and thin polymer membranes. Nonetheless, these techniques suffer from high cost, complex processes, difficulty in adjusting pattern features, sophistication, sensitivity, high time consumption, complex protocols, and the need for a careful operation [43–45]. All these obstacles will restrict the mass production of porous and flexible polymer membranes, specifically for large-scale energy harvesting and energy storage, where a large number of TENG devices with a high surface area and surface roughness must work together. To overcome these limitations, it is essential to develop cost-effective and mass production fabrication procedures to develop porous and flexible polymer membranes for novel TENG devices using cost-effective methods.

Herein, we used a novel, simple and convenient bar coating method for the mass production of flexible porous PU membrane. The fabricated PU membrane, along with PTFE, was used for the fabrication of a flexible and thin TENG device for mechanical energy harvesting. PU and PTFE were selected as triboelectric positive and triboelectric negative materials owing to their excellent electropositivity and electronegativity, respectively. The electrical performance of the fabricated TENG device was systematically investigated. The electricity produced from the TENG was also used to power LED and LCD to evaluate its real application. Compared with other PU-based TENG devices and their fabrication methods, the TENG device assembled using PU based on the currently developed novel fabrication method showed appreciable performance in terms of electrical

performance and mechanical energy harvesting. Based on our findings, we expect that the developed fabrication method will pave the way for the facile and scalable processing of PU for energy-harvesting applications.

2. Experimental

2.1. Materials

An aqueous dispersion of PU solution was purchased from Gabriel Advanced Materials Co., Ltd, Taiwan. The aqueous dispersion of PU solution comprises of PU dispersion formulation, foaming agents, surfactant, and crosslinking agent. A PTFE film (0.25 mm thickness) was purchased from Sanytle, Taiwan. Copper film (0.1 mm thickness) and Kapton tape were purchased from KWO-YI Ltd, Taipei, Taiwan. Prior to use, copper substrates were successively cleaned with acetone, 0.1 M sulfuric acid solution, and distilled water, followed by purging and blow-drying in nitrogen gas.

2.2. Fabrication of porous PU membranes with different thicknesses

PU membranes with 5, 20, and 40 μm thickness, named PU-5, PU-20, and PU-40, respectively, were prepared using a bar coating method. Initially, the as-received 49 wt% of PU aqueous dispersion solution was mechanically stirred for 10 min. Then, the mechanically stirred solution was drop-casted on a copper substrate and then manually bar coated with different wet gaps (RDS 10, RDS 40, and RDS 80) of bar coating rods to obtain PU membranes with the desired thickness. Finally, the bar-coated PU membranes were dried in an oven at 90 °C for 10 min. Additionally, 5 μm-thick PU membranes with 15, 30, and 60 μm average pore sizes (labeled as PU-5-15, PU-5-30, and PU-5-60) were also prepared by adjusting the amount of foaming agent and controlling the stirring speed. The fabrication process of PU membrane is schematically shown in Figure 1.

2.3. Fabrication of TENG device

For designing a contact-separation mode TENG device, a four-layer structure, *i.e.*, Cu, PU, PTFE, and Al foil, was used. PU was used as a positively charged triboelectric layer; commercially available PTFE film was used as a negatively charged triboelectric layer. Cu and Al were used as electrodes and serve as friction surfaces. PTFE film and porous PU membrane have opposite triboelectric charges and good contact, and they also serve as friction surfaces for the device. Circular-shaped TENG devices with 5 cm size were used to achieve electrical and output performance. The triboelectric layer's components were assembled with a separation distance of 5 mm using double-sided tape as a spacer.

2.4. Characterization

Surface morphologies of the PU membranes were characterized by field-emission scanning electron microscopy (FE-SEM, JEOL JSM-6500F, Akishima, Tokyo, Japan). A universal tester (QC-508M2, Cometech, Taichung, Taiwan) was used at room temperature to apply vertical impulse compression to the TENG device. The electrical responses of the fabricated PU membrane were measured using a Keithley source meter unit (SMU, Keithley 2400, Tektronix, Beaverton, OR, USA). The assembled device was placed under compression, where the force can be applied and controlled using a load cell. The force was applied using a load cell with a capacity of 1 to 1000 N (Cometech, Model BTS, J1927657, Capacity = 1 kN) at a fixed frequency of 0.15 Hz. The electrical response data were collected and analyzed using a computer.

3. Results and discussion

Figure 2a shows the assembly of the TENG device, comprising Cu, PU, PTFE, and Al layers. Cu and PTFE with a negative charge serve as negative triboelectric layers; on the other hand, PU and Al with

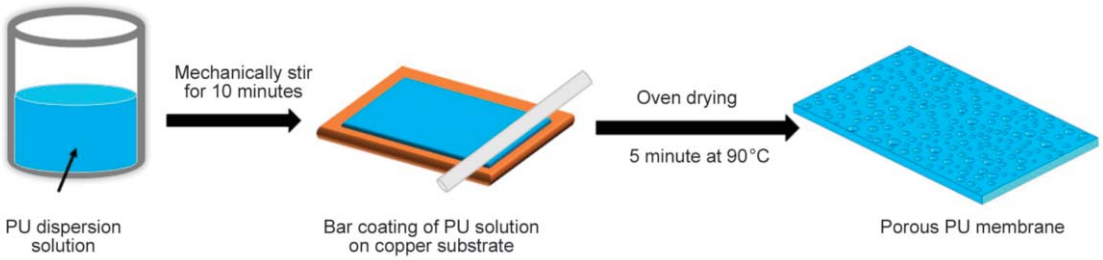

Figure 1. Schematic fabrication process of porous PU membrane.

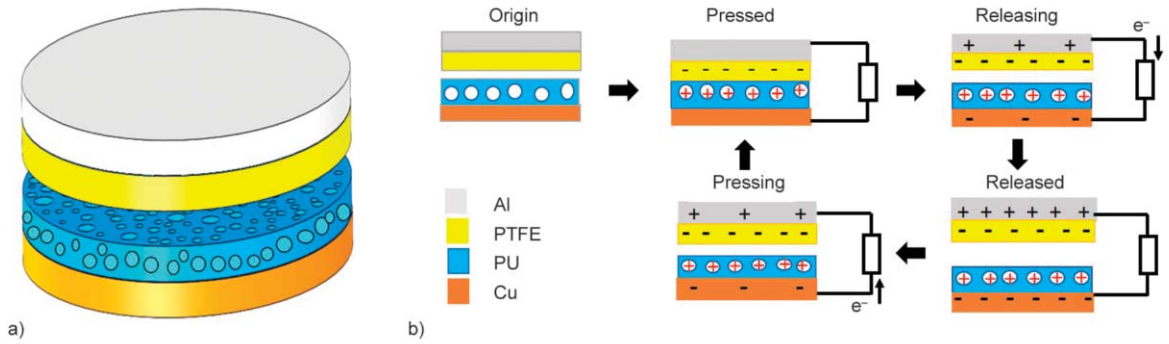

Figure 2. (a) Assembly of TENG device and (b) working mechanism of vertical contact separation mode of TENG device.

a positive charge serve as positive triboelectric layers. Generally, Al will work as both a positive and negative material. Figure 2b shows a schematic working mechanism of vertical contact separation mode novel TENG device.

The working mechanism and electrical power generation of fabricated TENG devices can be elucidated based on coupling effects, electrostatic induction, and conjunction of triboelectrification in the inner and outer layers of the device. In the initial state, a charge will not be generated either on the porous PU membrane or on the PTFE layer. When the two tribo-surfaces, *i.e.*, the porous PU membrane and PTFE layers, came into physical contact, the corresponding positive charges will be generated on the porous PU membrane, whereas negative charges will be generated on the PTFE layer based on the contact triboelectrification working mechanism. The generated positive and negative charges on the tribo-surfaces are due to the propensity of porous PU membrane to lose electrons and the propensity of PTFE film to gain electrons. At this stage, owing to the accumulation, the PTFE and PU surface electric charge density on the dielectric surface gradually increases and reaches its saturation level. Owing to the presence of pores in PU layer, electrical and surface charges are induced on the porous PU membrane surface. This type of tendency can also be ascertained on the basis of compression of pores generated on the PU membrane along with the associated electrostatic effects [20, 46]. Furthermore, on the surface of PU, positive electric charges can be efficiently preserved owing to the inherent insulating nature of PU. When two tribo-layers in a TENG device contact each other, the friction or the surface contact area between the two tribo-layers gradually increases [46, 47]. Furthermore, when the two contacting tribo-surfaces are releasing electrons, electrostatic interactions will increase, and charge transfer between tribo-layers will occur until the difference in the electrical potential generates positive current signals. The dielectric surface on the Al surface passes the electrons towards the PU membrane along with the external load until the electrostatic equilibrium between the PU and PTFE is established. On the other hand, the capacitance and surface area of TENG will gradually decrease during the release of pressure on the PU membrane, which in turn leads to the opposite current until it is fully released. Furthermore, when the triboelectric materials are contacting each other, an electrostatic field will drive the flow and transfer the electrons back to the top Al layer until it achieves the electrostatic equilibrium position. Thus, a single-cycle process of contact-separation mode of TENG can be achieved.

Figures 3a–3c shows the surface morphology and Figures 3d–3f depicts the cross-sectional images of fabricated porous PU membranes, *i.e.*, PU-5, PU-20, and PU-40 membranes. The obtained findings explicitly portray the porous morphological features and desired thickness of PU membranes. The average pore sizes of PU membranes were calculated to be 31.21±20.90 μm for PU-5, 33.65±23.59 μm for PU-20, and 37.19±26.65 μm for PU-40. Pore sizes were calculated by inserting the corresponding FESEM micrographs in Motic Images Plus 2.0 ML software. The increase in the average pore size of PU membranes with the increase in the thickness of PU can be attributed to the increase in interfacial distance and inference of PU membranes. Structures with various pore sizes (micro and macropores) of the PU will help in inducing additional charges for the device; moreover, they will augment the capacitance by reducing the dielectric film thickness of the membrane. All these features will enhance the electrical performance of the device [48–50].

The effect of porous PU membrane thickness on the electrical properties of TENG device was analyzed

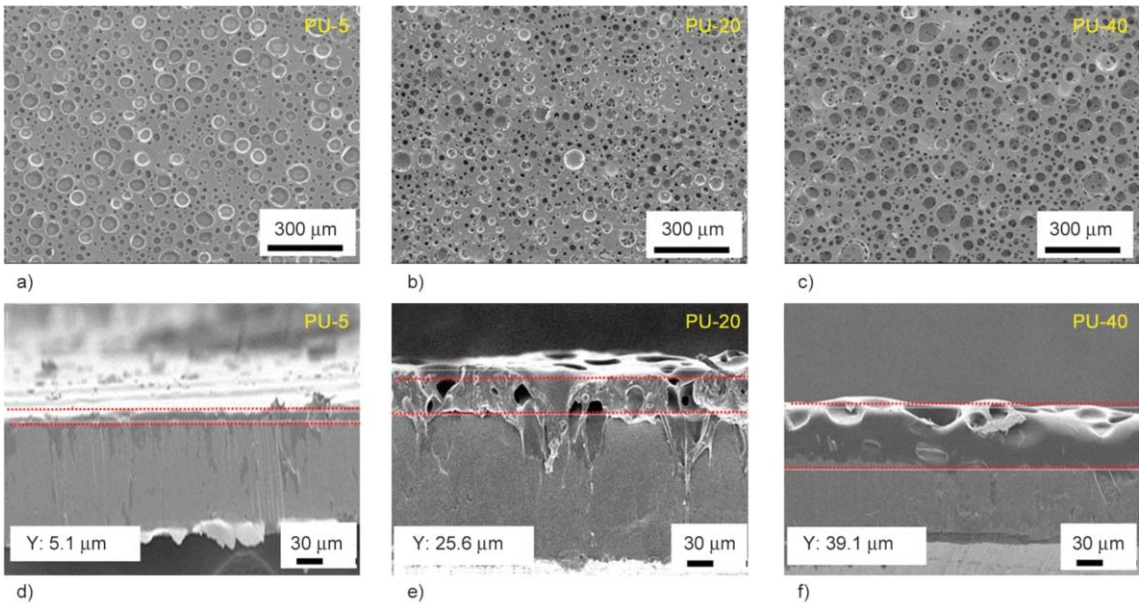

Figure 3. (a)–(c) FESEM surface morphologies and (d)–(f) cross-sectional FESEM images of PU-5, PU-20, and PU-40 membranes, respectively.

systematically. The effect of various thicknesses of PU membrane on the output voltage (Figure 4a) and current (Figure 4b) performance of TENG device at different force was studied. Among the various thicknesses, the PU-5 membrane showed better electrical performance of the output voltage was 26.3 V and output current was 0.78 µA. With the increasing thickness of the PU membrane, the electrical performance of the TENG device decreases due to the presence of a larger pore size or lower number of pores and lower surface area. Moreover, the electrical resistance of PU membranes with different thicknesses was also measured. PU-5 membrane presented the lowest electrical resistance of 0.312 Ω, while PU-20 and PU-40 membranes showed electrical resistance of 0.500 and 0.885 Ω, respectively. This further confirms that the effect of PU membrane thickness on the electrical performance of the TENG device. The obtained results indicate that the pore size and pore count of the PU membrane play a crucial role in the electrical performance and transfer of electrons in the TENG device. These results indicate that the TENG device fabricated with PU-5 has appreciable performance and was employed for further studies.

Furthermore, PU-5 membranes with various average pore sizes such as PU-5-15, PU-5-30, and PU-5-60 were fabricated to evaluate the effect of pore size

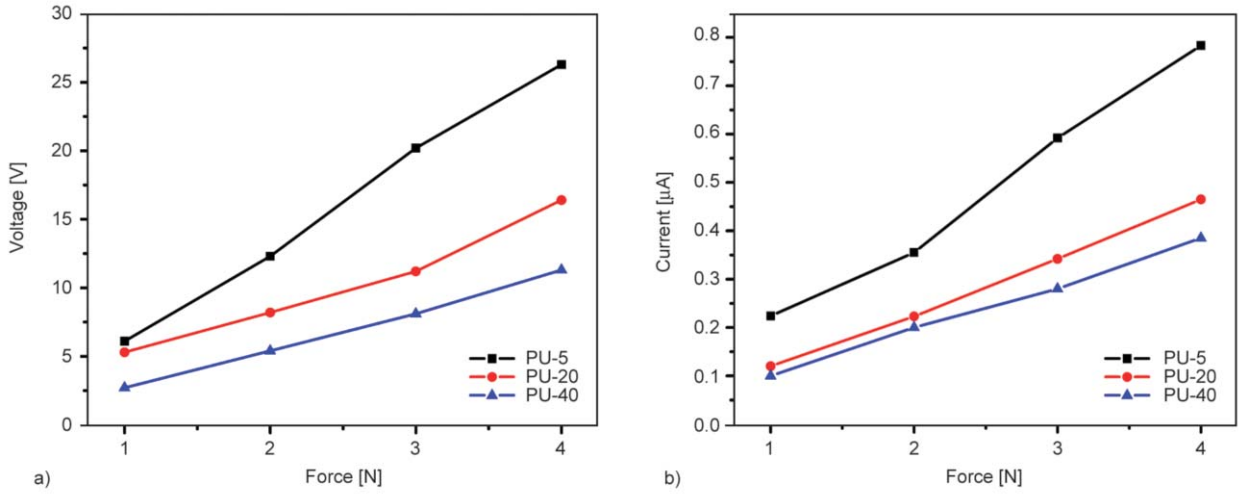

Figure 4. Electrical performance of fabricated TENG device with PU-5, PU-20, and PU-40 membranes with 30 µm pore size at a fixed frequency of 0.15 Hz. (a) output voltage and (b) current of various PU membranes with various thicknesses as a function of force.

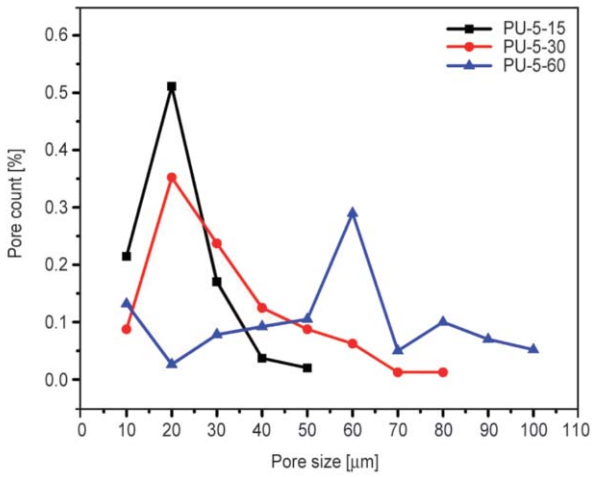

Figure 5. Variations in the pore sizes with respect to pore count of the PU-5-15, PU-5-30 and PU-5-60.

on the electrical performance of the TENG device. Figure 5 represents the variations in pore sizes with respect to the pore count of PU-5-15, PU-5-30, and PU-5-60. Among them, the PU-5-15 membrane has more pore count, which will help in enhancing the electrical performance of the TENG device by increasing the interfacial distance and by the proper exchange of current signals within the device. Figure 6a shows the surface morphological pores features. The average pore sizes for the PU membranes were calculated to be 16.92±9.45, 31.21±20.90, and 64.98±44.40 µm for PU-5-15, PU-5-30, and PU-5-60, respectively.

The observed electrical performance (voltage and current) of the TENG device fabricated with an increasing average pore size of PU membrane the maximum peak to peak voltage was 58.5 V and peak to peak current was 1.37 µA, 46.3 V and 0.86 µA, and 26.3 V and 0.68 µA for PU-5-15, PU-5-30, and PU-5-60, respectively (Figure 6b and 6c). With the increasing pore size of the PU membrane, the electrical performance of the TENG device decreases. This type of behavior can be attributed to a decrease in the surface area to volume ratio of PU and an increase in pore size. Compared to other average pore sizes of PU membranes, the average pore size of PU-5-15 achieved the highest electrical performance.

The electrical performance (voltage and current) of the TENG device fabricated with PU-5-15 was tested with increasing compression force from 1 to 15 N. Figure 7a shows the obtained electrical performance results. The voltage of the device increased with the

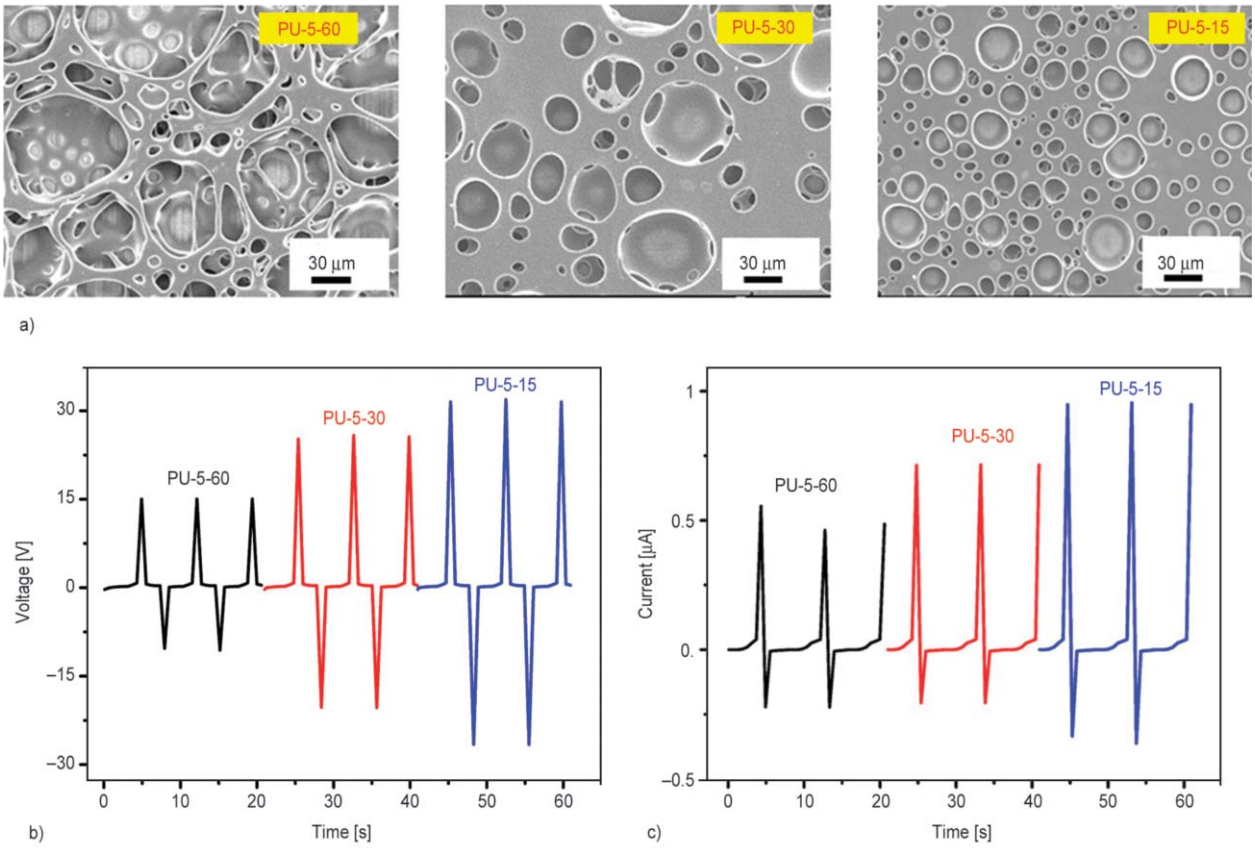

Figure 6. Electrical performance of fabricated TENG device. (a) FESEM images, and (b) output voltage and (c) current of PU-5 membrane with various average pore sizes PU-5-15, PU-5-30, and PU-5-60 at 4 N force.

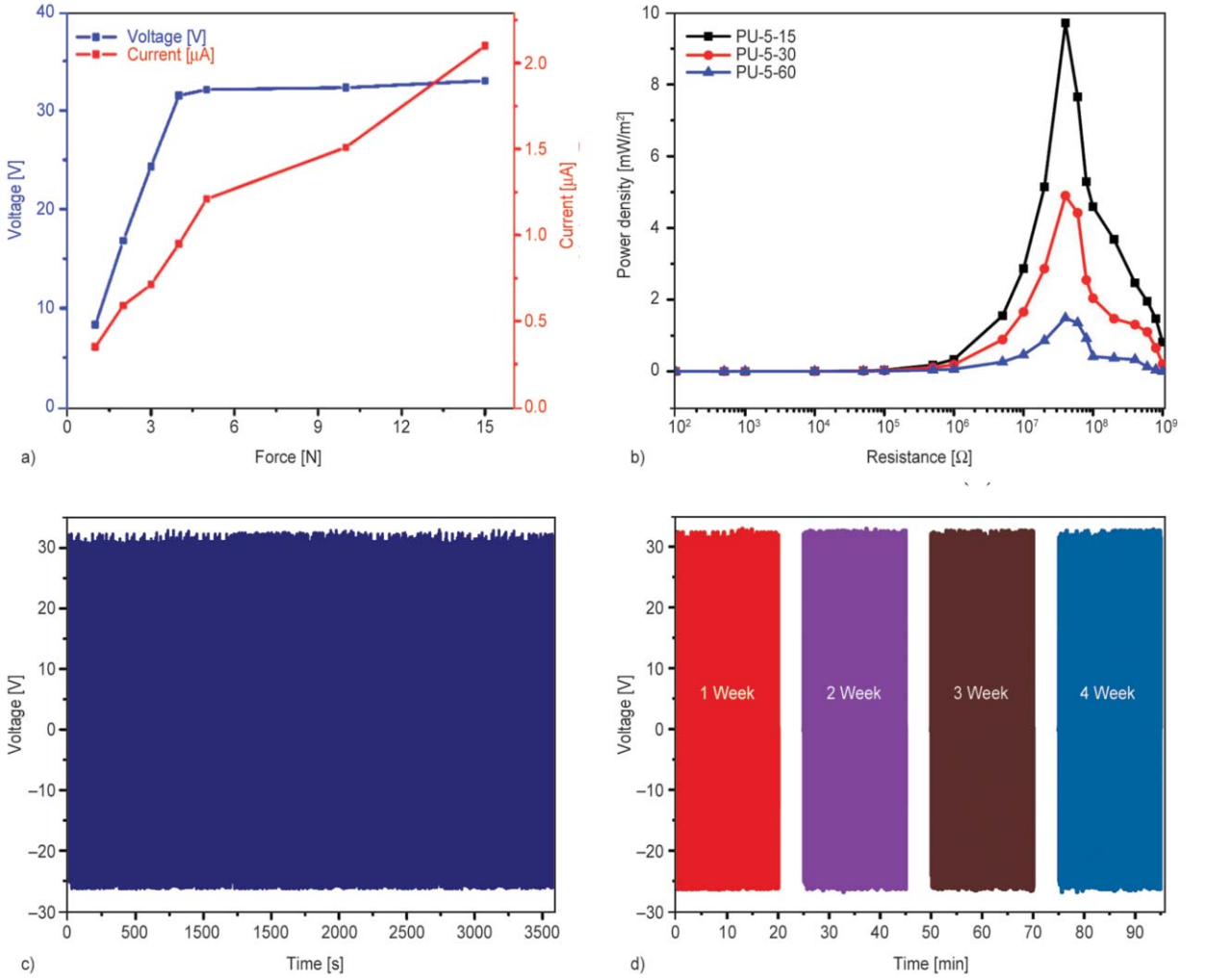

Figure 7. (a) Electrical performance of TENG device fabricated with PU-5-15, (b) peak power density of TENG device, (c) stability performance of TENG device for 3500 s (500 cycles), and (d) stability performance of TENG device for 4 weeks, respectively.

increase in compression force up to 5 N; the voltage did not increase with a further increase in compression force. This type of tendency can be attributed to the variation in capacitance, as the maximum voltage was achieved at 5 N. However, the current of the device gradually increases with the increase in compression force. These variations can be attributed to the pore size, surface roughness, and compressibility of PU membranes.

The maximum generated voltage and current were indeed necessary to determine the power generation efficiency of the fabricated TENG device. Therefore, the effective electrical performance of the TENG device fabricated with various average pore sizes of PU-5 membrane was measured by connecting the resistors with various resistance values (10^2 to 10^9 Ω) at an applied compression force of 4 N. It is evident that the maximum power density of TENG device depends on the short and open-circuit electrical performances. Therefore, based on the results obtained from the measured current and voltage of TENG device with various load resistances, power density was calculated ($P = I^2 \cdot R/A$) as shown in Figure 7b. The TENG device displayed lower power density values at the maximum and minimum load resistances. The maximum power densities of the PU-based TENG device with PU-5-15, PU-5-30, and PU-5-60 at a load resistance of 40 MΩ were estimated to be 9.7, 4.9, and 1.5 mW/m^2, respectively. The obtained load resistance of 40 MΩ was identified as the optimized load matching resistance for practical applications. TENG device with PU-5-15 showed the best power density.

The stability of the TENG device was evaluated by testing for 500 cycles under an applied compression force of 4 N. As shown in Figure 7c, the voltage of the fabricated device was uniform, and no distinguishable change was observed even after 500 cycles. The

surface characteristic features and relative pore density of PU membranes can be attributed to the stability of the device. The long-term stability of the device was also measured for four weeks, as illustrated in Figure 7d. While measuring the long-term stability, the device was stored at room temperature. The obtained stability results indicate that the TENG device fabricated with PU-5-15 has acceptable stability and appreciable structural durability.

To verify the electrical output performance and energy-harvesting efficiency of PU-5-15 TENG device, different confirmatory tests were executed. Electrical power generated from the TENG device fabricated with PU-5-15 membrane was further demonstrated for real-time practical applications to energize portable electronics. 24 green commercial LEDs connected in a series were instantaneously energized with high brightness in bright condition under hand tapping (photographs are shown in Figure 8a). A constant DC signal is needed to energize the electronic devices with low power. However, AC signals produced from the TENG device cannot be used to directly draw the electrical signals from the energy storage devices. Therefore, the electrical output performance generated from the TENG device was rectified using a bridge rectifier circuit. Figure 8b shows the time-charging cycle for various commercially available capacitors (1, 10, 22, 47 μF) using a PU-5-15 sample under the application of force provided by hand taping. The results indicate that the capacitors

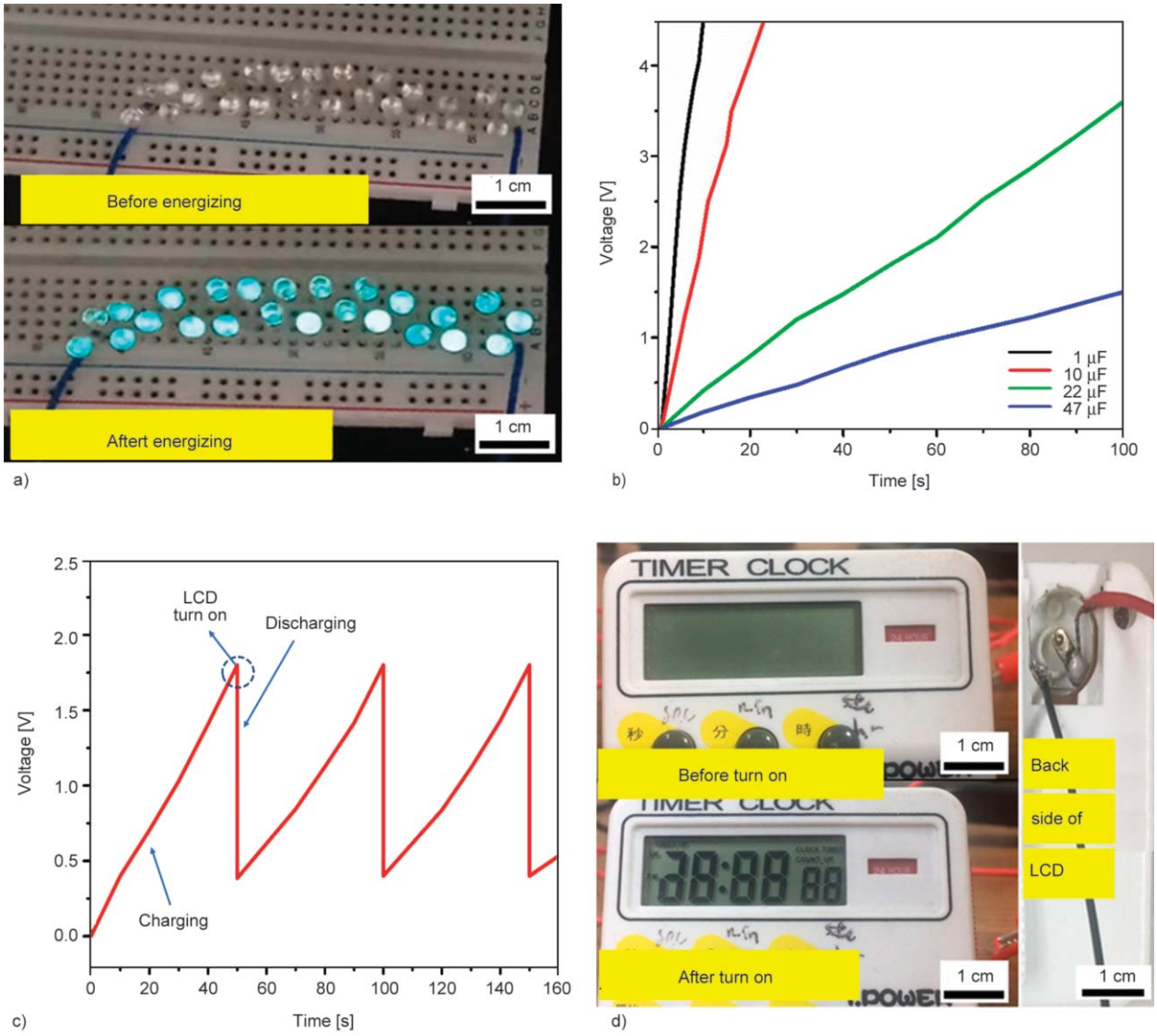

Figure 8. Applications of TENG device fabricated with PU-5-15 membrane. (a) 24 green commercial LEDs energized in a bright condition, (b) capacitor charging characteristics with various commercial capacitors. (c) voltage charging and discharging curve of a 22 μF capacitor underhand tapping force generated from the TENG device, and (d) images of LCD portable timer clock energized by the TENG device through a bridge rectifier and 22 μF capacitor.

with a low capacitance were charged very fast compared to those with a larger capacitance, and by extending the taping time up to 100 s, the capacitor with 22 μF can reach 3.6 V. This clearly shows that different capacitors can be charged by the rectified voltage and used as self-powered energy sources in electronic devices.

Additionally, the TENG device fabricated with PU-5-15 was used to glow the electrical display of a portable timer clock that consumes low power. Therefore, a bridge rectifier circuit was used to rectify the output voltage produced by the TENG device by storing the electrical voltage performance in the 22 μF capacitor. Figure 8c depicts the charging and discharging curves of the 22 μF capacitor. The voltage accumulated in the capacitor energized the electrical display of the portable timer clock within 51 s and glowed for 1 s after 187 taps, which is suitable for performing several right tests as shown in Figure 8d. The fabricated TENG device also presented stable charging and discharging cyclability that makes this device a promising potential candidate in real applications of charging electronic devices. Furthermore, the charging and discharging property of the prepared TENG device for 47 μF capacitor was also checked, and our device can energize it similarly after tapping for 190 s.

To further validate the real-time or practical applications of the TENG device, the device was placed on the palm of the hand, in between the elbow of the hand, and air was blown on the device using a hairdryer. Figure 9a shows the body movements performed with the TENG device. At the instant, when the palm of the hand is pressed with fingers, the elbow is bent, and air is blown on the device. The mechanical energies or pushing forces applied on the TENG device by the motion of pressing, bending, and blowing can be efficiently converted into electricity. The generated electrical output voltage of PU-based TENG device on the palm of the hand (4.3 V), elbow (3.3 V), and air blown (1.5 V) are shown in Figures 9b, 9c, and 9d, respectively. These confirmatory electrical performance results of real-time applications authenticate that the fabricated TENG device can be used as a promising and significant candidate for driving low-power electronic devices.

It is worth mentioning that, when compared with other PU membrane-based TENG devices and their

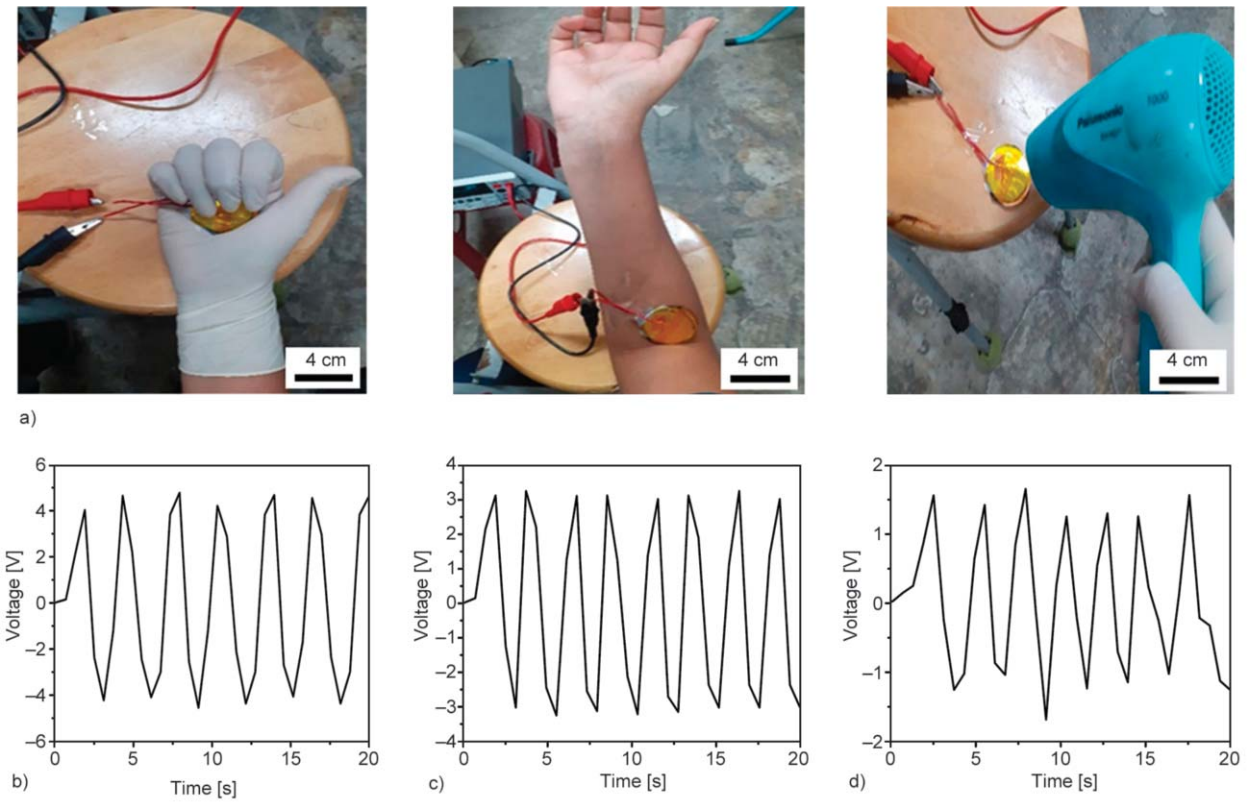

Figure 9. Real-time applications of TENG device fabricated with PU-5-15 membrane for harvesting the mechanical energy when placed on the palm of the hand, elbow, and with the blowing of air on the device with a dryer. (a) photographs of body movements and (b–d) their corresponding electrical performance results.

Table 1. Comparison of electrical performance of PU-based TENG devices.

Preparation method	Area [cm^2]	Thickness [µm]	Test method	Peak to peak voltage [V]	Peak to peak current [µA]	Power density [mW/m^2]	Reference
Commercial	14.5	10000	Weight sensor & different strains	12.00	0.016	–	[51]
CO_2 and N_2 foaming	2	10000	Different objects	43.00	–	–	[52]
Collected from garbage bin	9	200	Cyclic compressive force (12 N)	44.00	0.289	3.2	[53]
Electrospun	5	80	Pushing machine 5 N, 8 Hz	6.63	0.970	9.0	[54]
Bar coating	19.6	5	Compression (4 N)	58.50	1.370	9.7	This work

fabrication methods, the TENG device assembled using a PU membrane based on the currently developed method showed appreciable performance for electrical voltage, current, and power density production [51–54], as shown in Table 1.

4. Conclusions

In this study, we developed a cost-effective and scalable method for the fabrication of lightweight, flexible, thin, and porous PU membranes as a potential triboelectric materials for a PU-based TENG device. Importantly, the thickness and pore size of the PU membrane can be adjusted. The TENG device fabricated with PU-5-15 membrane showed better performance by generating the maximum peak to peak output voltage of 58.5 V and a corresponding peak to peak current of 1.37 µA at 4 N and power density of 9.7 mW/m^2. The device was systematically used to glow 24 green commercial LEDs in brighter condition connected in series and to turn on the LCD of a portable timer clock within 51 s and glow for 1 s after 187 taps. The developed TENG device also exhibited stable cyclic charging and discharging property that is very important for real applications. Furthermore, the TENG device was used to harvest mechanical energies with triboelectric effects for real-time and practical applications. The studied practical applications significantly demonstrated that the fabricated TENG device efficiently converts mechanical movements into electricity. The developed industrially compatible method will pave the way for the facile and scalable industrial processing of PU membranes, which has a significant promise in energy-harvesting and storage applications.

Acknowledgements

We would like to acknowledge the Ministry of Science and Technology of Taiwan, ROC, for financially supporting part of this work, under contract number: MOST 108-2221-E-011-040-MY2.

References

[1] Gielen D., Boshell F., Saygin D.: Climate and energy challenges for materials science. Nature Materials, **15**, 117–120 (2016). https://doi.org/10.1038/nmat4545

[2] Mintken M., Schweichel M., Schröder S., Kaps S., Carstensen J., Mishra Y. K., Strunskus T., Faupel F., Adelung R.: Nanogenerator and piezotronic inspired concepts for energy efficient magnetic field sensors. Nano Energy, **56**, 420–425 (2019). https://doi.org/10.1016/j.nanoen.2018.11.031

[3] Chu S., Majumdar A.: Opportunities and challenges for a sustainable energy future. Nature, **488**, 294–303 (2012). https://doi.org/10.1038/nature11475

[4] Guo H., Pu X., Chen J., Meng Y., Yeh M-H., Liu G., Tang Q., Chen B., Liu D., Qi S., Wu C., Hu C., Wang J., Wang Z. L.: A highly sensitive, self-powered triboelectric auditory sensor for social robotics and hearing aids. Science Robotics, **3**, eaat2516/1–eaat2516/9 (2018). https://doi.org/10.1126/scirobotics.aat2516

[5] Dao V-D.: An experimental exploration of generating electricity from nature-inspired hierarchical evaporator: The role of electrode materials. Science of The Total Environment, **759**, 143490/1–143490/6 (2021). https://doi.org/10.1016/j.scitotenv.2020.143490

[6] Chen C. Y., Tsai C. Y., Xu M. H., Wu C. T., Huang C. Y., Lee T. H., Fuh Y. K.: A fully encapsulated piezoelectric–triboelectric hybrid nanogenerator for energy harvesting from biomechanical and environmental sources. Express Polymer Letters, **13**, 533–542 (2019). https://doi.org/10.3144/expresspolymlett.2019.45

[7] Yan C., Gao Y., Zhao S., Zhang S., Zhou Y., Deng W., Li Z., Jiang G., Jin L., Tian G., Yang T., Chu X., Xiong D., Wang Z., Li Y., Yang W., Chen J.: A linear-to-rotary hybrid nanogenerator for high-performance wearable biomechanical energy harvesting. Nano Energy, **67**, 104235/1–104235/5 (2020). https://doi.org/10.1016/j.nanoen.2019.104235

[8] Jin L., Xiao X., Deng W., Nashalian A., He D., Raveendran V., Yan C., Su H., Chu X., Yang T., Li W., Yang W., Chen J.: Manipulating relative permittivity for high-performance wearable triboelectric nanogenerators. Nano Letters, **20**, 6404–6411 (2020). https://doi.org/10.1021/acs.nanolett.0c01987

[9] Zhou Z., Weng L., Tat T., Libanori A., Lin Z., Ge L., Yang J., Chen J.: Smart insole for robust wearable biomechanical energy harvesting in harsh environments. ACS Nano, **14**, 14126–14133 (2020). https://doi.org/10.1021/acsnano.0c06949

[10] Deng W., Zhou Y., Zhao X., Zhang S., Zou Y., Xu J., Yeh M-H., Guo H., Chen J.: Ternary electrification layered architecture for high-performance triboelectric nanogenerators. ACS Nano, **14**, 9050–9058 (2020). https://doi.org/10.1021/acsnano.0c04113

[11] Zou Y., Xu J., Fang Y., Zhao X., Zhou Y., Chen J.: A hand-driven portable triboelectric nanogenerator using whirligig spinning dynamics. Nano Energy, **83**, 105845/1–105845/6 (2021). https://doi.org/10.1016/j.nanoen.2021.105845

[12] Yin H., Hui K. S., Zhao X., Mei S., Lv X., Hui K. N., Chen J.: Eco-friendly synthesis of self-supported n-doped Sb_2S_3-carbon fibers with high atom utilization and zero discharge for commercial full lithium-ion batteries. ACS Applied Energy Materials, **3**, 6897–6906 (2020). https://doi.org/10.1021/acsaem.0c00984

[13] Chen G., Li Y., Bick M., Chen J.: Smart textiles for electricity generation. Chemical Reviews, **120**, 3668–3720 (2020). https://doi.org/10.1021/acs.chemrev.9b00821

[14] Dao V-D., Vu N. H., Choi H-S.: All day limnobium laevigatum inspired nanogenerator self-driven *via* water evaporation. Journal of Power Sources, **448**, 227388/1–227388/7 (2020). https://doi.org/10.1016/j.jpowsour.2019.227388

[15] Gubbi J., Buyya R., Marusic S., Palaniswami M.: Internet of things (IoT): A vision, architectural elements, and future directions. Future Generation Computer Systems, **29**, 1645–1660 (2013). https://doi.org/10.1016/j.future.2013.01.010

[16] Karan S. K., Maiti S., Lee J. H., Mishra Y. K., Khatua B. B., Kim J. K.: Recent advances in self-powered tribo-/piezoelectric energy harvesters: All-in-one package for future smart technologies. Advanced Functional Materials, **30**, 2004446/1–2004446/52 (2020). https://doi.org/10.1002/adfm.202004446

[17] Nehra M., Dilbaghi N., Marrazza G., Kaushik A., Abolhassani R., Mishra Y. K., Kim K. H., Kumar S.: 1D semiconductor nanowires for energy conversion, harvesting and storage applications. Nano Energy, **76**, 104991/1–104991/25 (2020). https://doi.org/10.1016/j.nanoen.2020.104991

[18] Bauer S., Bauer-Gogonea S., Graz I., Kaltenbrunner M., Keplinger C., Schwödiauer R.: 25th anniversary article: A soft future: From robots and sensor skin to energy harvesters. Advanced Materials, **26**, 149–162 (2014). https://doi.org/10.1002/adma.201303349

[19] Fan F-R., Tian Z-Q., Wang Z. L.: Flexible triboelectric generator. Nano Energy, **1**, 328–334 (2012). https://doi.org/10.1016/j.nanoen.2012.01.004

[20] Bui V-T., Oh J-H., Kim J-N., Zhou Q., Huynh D. P., Oh I-K.: Nest-inspired nanosponge-Cu woven mesh hybrid for ultrastable and high-power triboelectric nanogenerator. Nano Energy, **71**, 104561/1–104561/9 (2020). https://doi.org/10.1016/j.nanoen.2020.104561

[21] Sahu M., Vivekananthan V., Hajra S., Khatua D. K., Kim S-J.: Porosity modulated piezo-triboelectric hybridized nanogenerator for sensing small energy impacts. Applied Materials Today, **22**, 100900/1–100900/10 (2021). https://doi.org/10.1016/j.apmt.2020.100900

[22] Wang Z. L.: Triboelectric nanogenerators as new energy technology for self-powered systems and as active mechanical and chemical sensors. ACS Nano, **7**, 9533–9557 (2013). https://doi.org/10.1021/nn404614z

[23] Manchi P., Graham S. A., Dudem B., Patnam H., Yu J. S.: Improved performance of nanogenerator *via* synergetic piezo/triboelectric effects of lithium niobate microparticles embedded composite films. Composites Science and Technology, **201**, 108540/1–108540/10 (2021). https://doi.org/10.1016/j.compscitech.2020.108540

[24] Xu J., Zou Y., Nashalian A., Chen J.: Leverage surface chemistry for high-performance triboelectric nanogenerators. Frontiers in Chemistry, **8**, 577327/1–577327/23 (2020). https://doi.org/10.3389/fchem.2020.577327

[25] Zou Y., Raveendran V., Chen J.: Wearable triboelectric nanogenerators for biomechanical energy harvesting. Nano Energy, **77**, 105303/1–105303/19 (2020). https://doi.org/10.1016/j.nanoen.2020.105303

[26] Zou Y., Libanori A., Xu J., Nashalian A., Chen J.: Triboelectric nanogenerator enabled smart shoes for wearable electricity generation. Research, **2020**, 7158953/1–7158953/20 (2020). https://doi.org/10.34133/2020/7158953

[27] Zan G., Wu T., Hu P., Zhou Y., Zhao S., Xu S., Chen J., Cui Y., Wu Q.: An approaching-theoretical-capacity anode material for aqueous battery: Hollow hexagonal prism Bi_2O_3 assembled by nanoparticles. Energy Storage Materials, **28**, 82–90 (2020). https://doi.org/10.1016/j.ensm.2020.02.027

[28] Fan F. R., Luo J., Tang W., Li C., Zhang C., Tian Z., Wang Z. L.: Highly transparent and flexible triboelectric nanogenerators: Performance improvements and fundamental mechanisms. Journal of Materials Chemistry A, **2**, 13219–13225 (2014). https://doi.org/10.1039/C4TA02747G

[29] Surmenev R. A., Chernozem R. V., Pariy I. O., Surmeneva M. A.: A review on piezo- and pyroelectric responses of flexible nano- and micropatterned polymer surfaces for biomedical sensing and energy harvesting applications. Nano Energy, **79**, 105442/1–105442/24 (2021). https://doi.org/10.1016/j.nanoen.2020.105442

[30] Wu C. M., Chou M. H.: Acoustic-electric conversion and piezoelectric properties of electrospun polyvinylidene fluoride/silver nanofibrous membranes. Express Polymer Letters, **14**, 103–114 (2020). https://doi.org/10.3144/expresspolymlett.2020.10

[31] Wu C-M., Chou M-H., Chala T. F., Shimamura Y., Murakami R-I.: Infrared-driven poly(vinylidene difluoride)/tungsten oxide pyroelectric generator for non-contact energy harvesting. Composites Science and Technology, **178**, 26–32 (2019). https://doi.org/10.1016/j.compscitech.2019.05.004

[32] Zhou Z., Padgett S., Cai Z., Conta G., Wu Y., He Q., Zhang S., Sun C., Liu J., Fan E., Meng K., Lin Z., Uy C., Yang J., Chen J.: Single-layered ultra-soft washable smart textiles for all-around ballistocardiograph, respiration, and posture monitoring during sleep. Biosensors and Bioelectronics, **155**, 112064/1–112064/8 (2020). https://doi.org/10.1016/j.bios.2020.112064

[33] Tat T., Libanori A., Au C., Yau A., Chen J.: Advances in triboelectric nanogenerators for biomedical sensing. Biosensors and Bioelectronics, **171**, 112714/1–112714/29 (2021). https://doi.org/10.1016/j.bios.2020.112714

[34] Meng K., Zhao S., Zhou Y., Wu Y., Zhang S., He Q., Wang X., Zhou Z., Fan W., Tan X., Yang J., Chen J.: A wireless textile-based sensor system for self-powered personalized health care. Matter, **2**, 896–907 (2020). https://doi.org/10.1016/j.matt.2019.12.025

[35] Zhou Z., Chen K., Li X., Zhang S., Wu Y., Zhou Y., Meng K., Sun C., He Q., Fan W., Fan E., Lin Z., Tan X., Deng W., Yang J., Chen J.: Sign-to-speech translation using machine-learning-assisted stretchable sensor arrays. Nature Electronics, **3**, 571–578 (2020). https://doi.org/10.1038/s41928-020-0428-6

[36] Zhang G., Zhao P., Zhang X., Han K., Zhao T., Zhang Y., Jeong C. K., Jiang S., Zhang S., Wang Q.: Flexible three-dimensional interconnected piezoelectric ceramic foam based composites for highly efficient concurrent mechanical and thermal energy harvesting. Energy and Environmental Science, **11**, 2046–2056 (2018). https://doi.org/10.1039/C8EE00595H

[37] Wang Y., Yang Y., Wang Z. L.: Triboelectric nanogenerators as flexible power sources. npj Flexible Electronics, **1**, 10/1–10/10 (2017). https://doi.org/10.1038/s41528-017-0007-8

[38] Li X., Jiang C., Zhao F., Lan L., Yao Y., Yu Y., Ping J., Ying Y.: Fully stretchable triboelectric nanogenerator for energy harvesting and self-powered sensing. Nano Energy, **61**, 78–85 (2019). https://doi.org/10.1016/j.nanoen.2019.04.025

[39] Hwang B-U., Lee J-H., Trung T. Q., Roh E., Kim D-I., Kim S-W., Lee N-E.: Transparent stretchable self-powered patchable sensor platform with ultrasensitive recognition of human activities. ACS Nano, **9**, 8801–8810 (2015). https://doi.org/10.1021/acsnano.5b01835

[40] Yi F., Wang J., Wang X., Niu S., Li S., Liao Q., Xu Y., You Z., Zhang Y., Wang Z. L.: Stretchable and waterproof self-charging power system for harvesting energy from diverse deformation and powering wearable electronics. ACS Nano, **10**, 6519–6525 (2016). https://doi.org/10.1021/acsnano.6b03007

[41] Mi H-Y., Jing X., Cai Z., Liu Y., Turng L-S., Gong S.: Highly porous composite aerogel based triboelectric nanogenerators for high performance energy generation and versatile self-powered sensing. Nanoscale, **10**, 23131–23140 (2018). https://doi.org/10.1039/C8NR05872E

[42] Duan S., Wang Z., Zhang L., Liu J., Li C.: A highly stretchable, sensitive, and transparent strain sensor based on binary hybrid network consisting of hierarchical multiscale metal nanowires. Advanced Materials Technologies, **3**, 1800020/1–1800020/8 (2018). https://doi.org/10.1002/admt.201800020

[43] Zhang X-S., Han M-D., Wang R-X., Zhu F-Y., Li Z-H., Wang W., Zhang H-X.: Frequency-multiplication high-output triboelectric nanogenerator for sustainably powering biomedical microsystems. Nano Letters, **13**, 1168–1172 (2013). https://doi.org/10.1021/nl3045684

[44] Zhang X-S., Han M-D., Wang R-X., Meng B., Zhu F-Y., Sun X-M., Hu W., Wang W., Li Z-H., Zhang H-X.: High-performance triboelectric nanogenerator with enhanced energy density based on single-step fluorocarbon plasma treatment. Nano Energy, **4**, 123–131 (2014). https://doi.org/10.1016/j.nanoen.2013.12.016

[45] Zhu Y., Yang B., Liu J., Wang X., Wang L., Chen X., Yang C.: A flexible and biocompatible triboelectric nanogenerator with tunable internal resistance for powering wearable devices. Scientific Reports, **6**, 22233/1–22233/10 (2016). https://doi.org/10.1038/srep22233

[46] Zhang H., Lu Y., Ghaffarinejad A., Basset P.: Progressive contact-separate triboelectric nanogenerator based on conductive polyurethane foam regulated with a Bennet doubler conditioning circuit. Nano Energy, **51**, 10–18 (2018). https://doi.org/10.1016/j.nanoen.2018.06.038

[47] Graham S. A., Dudem B., Patnam H., Mule A. R., Yu J. S.: Integrated design of highly porous cellulose-loaded polymer-based triboelectric films toward flexible, humidity-resistant, and sustainable mechanical energy harvesters. ACS Energy Letters, **5**, 2140–2148 (2020). https://doi.org/10.1021/acsenergylett.0c00635

[48] Lee K. Y., Chun J., Lee J-H., Kim K. N., Kang N-R., Kim J-Y., Kim M. H., Shin K-S., Gupta M. K., Baik J. M., Kim S-W.: Hydrophobic sponge structure-based triboelectric nanogenerator. Advanced Materials, **26**, 5037–5042 (2014). https://doi.org/10.1002/adma.201401184

[49] Jang D., Kim Y., Kim T. Y., Koh K., Jeong U., Cho J.: Force-assembled triboelectric nanogenerator with high-humidity-resistant electricity generation using hierarchical surface morphology. Nano Energy, **20**, 283–293 (2016). https://doi.org/10.1016/j.nanoen.2015.12.021

[50] Zheng Q., Fang L., Guo H., Yang K., Cai Z., Meador M. A. B., Gong S.: Highly porous polymer aerogel film-based triboelectric nanogenerators. Advanced Functional Materials, **28**, 1706365/1–1706365/9 (2018). https://doi.org/10.1002/adfm.201706365

[51] Zhang S. L., Lai Y-C., He X., Liu R., Zi Y., Wang Z. L.: Auxetic foam-based contact-mode triboelectric nanogenerator with highly sensitive self-powered strain sensing capabilities to monitor human body movement. Advanced Functional Materials, **27**, 1606695/1–1606695/10 (2017). https://doi.org/10.1002/adfm.201606695

[52] Li H., Sinha T. K., Oh J. S., Kim J. K.: Soft and flexible bilayer thermoplastic polyurethane foam for development of bioinspired artificial skin. ACS Applied Materials and Interfaces, **10**, 14008–14016 (2018). https://doi.org/10.1021/acsami.8b01026

[53] Khandelwal G., Chandrasekhar A., Alluri N. R., Vivekananthan V., Raj N. P. M. J., Kim S-J.: Trash to energy: A facile, robust and cheap approach for mitigating environment pollutant using household triboelectric nanogenerator. Applied Energy, **219**, 338–349 (2018). https://doi.org/10.1016/j.apenergy.2018.03.031

[54] Oh H. J., Bae J. H., Park Y. K., Song J., Kim D. K., Lee W., Kim M., Heo K. J., Kim Y., Kim S. H., Yeang B. J., Lim S. J.: A highly porous nonwoven thermoplastic polyurethane/polypropylene-based triboelectric nanogenerator for energy harvesting by human walking. Polymers, **12**, 1044/1–1044/11 (2020). https://doi.org/10.3390/polym12051044